

COBALT-RICH AMORPHOUS RIBBONS FOR STRAIN SENSING IN CIVIL ENGINEERING

L. Kraus, F. Fendrych, P. Švec^a, J. Bydžovský^b, M Kollár^b

Institute of Physics ASCR, Na Slovance 2, CZ-18221 Praha, Czech Republic

^aInstitute of Physics SAS, Dúbravská cesta 9, SK-84228 Bratislava, Slovakia

^bSlovak Technical University, Ilkovičova 3, SK-81219 Bratislava, Slovakia

Magnetoelastic properties of amorphous $\text{Co}_{71-x}\text{Fe}_x\text{Cr}_7\text{Si}_8\text{B}_{14}$ ($2 \leq x \leq 12$) and $\text{Co}_{74}\text{Ni}_6\text{B}_{20}$ ribbons, prepared by the planar flow casting, were investigated. Appropriate heat treatment was used to optimize the properties and to improve the strain sensor performance. Stress-annealing induces hard-ribbon-axis magnetic anisotropy and regular domain structure perpendicular to ribbon length. The magnetization reversal takes place by the moment rotation with the hysteresis loops linear nearly up to saturation and very low coercive field. The influence of applied stress on the domain structures, hysteresis loops and AC permeability μ was investigated. The behavior depends on the sign and magnitude of magnetostriction constant. For $\lambda_s < 0$ the permeability decreases with applied stress, but the domain structure practically does not change. In materials with $\lambda_s > 0$ the permeability increases and above the critical stress, where the anisotropy changes to the easy-ribbon-axis one, the longitudinal domain structure is observed and the hysteresis loops become rectangular. In low magnetostrictive alloys ($x = 2$ and 4) the AC reluctivity (μ^{-1}), measured at 5 kHz, is nearly linear function of applied stress. The strain sensors based on these materials show good linearity in a wide range of measured strain, low mechanical hysteresis and low sensitivity to stray magnetic fields.

(Received February 14, 2002; accepted 15 May 2002)

Keywords: Amorphous systems, Soft magnetic, Magnetomechanical coupling, Strain sensor

1. Introduction

Metallic glasses are interesting materials for many technical applications. Magnetic softness in combination with unique mechanical properties is particularly suitable for strain sensors [1]. The sensitivity of magnetoelastic strain sensors is thousand times higher in comparison with the resistive (wire) gauges. Their performance is based on the change of magnetic permeability with applied stress. Both, Fe-rich or Co-rich alloys with positive or negative magnetostriction, can be used for this purpose. Very sensitive strain sensors (with the figure of merit up to 5×10^5) were obtained using field-annealed Fe-rich amorphous ribbons with a high positive magnetostriction [2]. Nevertheless, they could be used only for smaller strains due to permeability saturation. To increase the range of measurements, as-quenched Co-Ni based alloys with negative magnetostriction were used [3]. Application of magnetoelastic sensors for the strain and load measurements in civil constructions, besides the high corrosion resistance, requires the small temperature coefficient and a wide range of measurable strains up to 2000 ppm (microstrains). To satisfy these conditions amorphous CoFeCrSiB alloys with higher content of Cr (7 at.%) and small magnetostriction constant were investigated in this work.

Special heat treatments of as-cast ribbons were used to improve the performance of strain sensors. It is known that the best magnetoelastic response is obtained if magnetization takes place by pure moment rotations [4]. For longitudinally magnetized ribbons this condition is obtained when the anisotropy easy axis is perpendicular to the ribbon length. In Co-rich amorphous alloys the transversal

magnetic anisotropy can be induced by annealing under tensile stress [5]. It will be shown that by stress-annealing of CoFeCrSiB alloys good materials, which can be used as yokes of inductive sensors for strain measurements in civil engineering, can be produced.

2. Experimental

Amorphous $\text{Co}_{71-x}\text{Fe}_x\text{Cr}_7\text{Si}_8\text{B}_{14}$ ribbons (with $x = 2, 3.3, 4, 6, 8$ and 12), 6 mm wide and about 20 μm thick, were prepared by the planar flow-casting. The annealing was done in a radiation furnace with the temperature plateau about 14 cm along its axis. For the stress-annealing a weight was applied to one of the cold ends of the sample. A PC controlled DC hysteresis loop tracer was used for the hysteresis loops measurement. The loops with or without applied stress were measured on 40 cm long straight samples with the pick-up coil 3 cm long placed at the center of the sample.

Domain structures on the shiny sides of ribbons were observed by scanning electron microscope JEOL Superprobe JXA-733 using the type II magnetic contrast of backscattered electrons [6]. The sample 7 cm long was placed in a special holder in which the tensile stress up to 800 MPa could be applied by means of a brass spring. No magnetic field was applied to the sample. The sample plane was tilted with respect to the electron beam around the longitudinal or transversal axis so that either longitudinal (L) or transversal (T) magnetic contrast could be observed.

Table 1. The parameters of as-quenched CoFeCrSiB amorphous ribbons (t thickness, J_s saturation polarization, J_r/J_s remanence to saturation ratio, H_c coercive force, W magnetizing work, λ_s magnetostriction constant).

Composition	t [μm]	J_s [T]	J_r/J_s	H_c [A/m]	W [J/m ³]	$10^6 \times \lambda_s$
$\text{Co}_{69}\text{Fe}_2\text{Cr}_7\text{Si}_8\text{B}_{14}$	19.7	0.56	0.32	2.9	12.4	-1.03
$\text{Co}_{67.7}\text{Fe}_{3.3}\text{Cr}_7\text{Si}_8\text{B}_{14}$	21.7	0.59	0.015	0.6	7.0	-0.46
$\text{Co}_{67}\text{Fe}_4\text{Cr}_7\text{Si}_8\text{B}_{14}$	17.0	0.58	0.12	0.4	5.3	+
$\text{Co}_{65}\text{Fe}_6\text{Cr}_7\text{Si}_8\text{B}_{14}$	22.1	0.54	0.12	2.6	22.3	+
$\text{Co}_{63}\text{Fe}_8\text{Cr}_7\text{Si}_8\text{B}_{14}$	27.2	0.62	0.11	2.7	45.2	+
$\text{Co}_{59}\text{Fe}_{12}\text{Cr}_7\text{Si}_8\text{B}_{14}$	20.5	0.72	0.13	3.7	60.0	+

The AC permeability of 30 cm long ribbons was measured at frequency of 5 kHz in a 34 cm long solenoid. All measurements were performed at the sine waveform of flux density with a constant amplitude (B_m) while the applied stress was changed. The range of stress up to 375 MPa is identical with strain $\varepsilon \approx 2000$ ppm, supposing the value of Young's modulus $E = 185$ GPa. Some selected samples were then used as a core of a two-coil strain sensor.

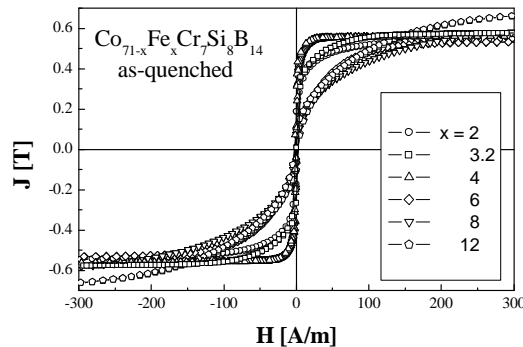


Fig. 1. Hysteresis loops of as-quenched $\text{Co}_{71-x}\text{Fe}_x\text{Cr}_7\text{Si}_8\text{B}_{14}$ ribbons.

3. Magnetoelastic properties

The ribbon thickness and basic magnetic parameters of as-quenched ribbons are summarized in table 1. Their hysteresis loops are shown in Fig.1. The loops are rounded with low remanence-to-saturation ratio and low coercive force. This indicates that magnetization reversal is determined mainly by local anisotropies due to inhomogeneous internal stresses. The saturation polarization J_s slightly increases with Fe content x (see Table 1). Both the coercive force H_c and the magnetizing work W (the area above the hysteresis loop) show distinct minima close to zero magnetostriction ($x \approx 4$). The magnetostriction constant λ_s can be estimated from the stress dependence $W(\sigma)$. For samples with $\lambda_s > 0$ $W(\sigma)$ rapidly decreases to 0 while for $\lambda_s < 0$ it increases and becomes linear for sufficiently high σ . The negative magnetostriction constant were calculated from the formula $\lambda_s = -2/3 dW/d\sigma$. The values of λ_s for alloys with $x \geq 4$ could not be determined in this way. The domain structures of as-quenched ribbons show the irregular “stress-induced pattern” characteristic for low magnetostriuctive amorphous ribbons. With increasing applied tensile stress the structures gradually change to wide stripe domains either parallel or perpendicular to the ribbon axis, depending on the sign of λ_s .

Stress-annealing for 1 hour with different annealing temperatures revealed that 350°C was an optimum annealing temperature for obtaining uniform transversal anisotropy without any traces of sample crystallization. Then samples were stress-annealed for 1 hour at 350°C with different applied stress (up to 700 MPa). The anisotropy constant of induced magnetic anisotropy, with the easy plane perpendicular to the ribbon axis, is proportional to the stress applied during the annealing, but practically independent of Fe content x . The domain structures of stress-annealed samples show wide stripe domains perpendicular to the ribbon axis. The domain walls usually show the zigzag structure, typical for the easy-plane anisotropy [7]. For the alloys with $x = 2$ and 4 the zigzags are more pronounced than for the ribbons with higher positive λ_s . When stress is applied to the sample, the domain structure changes depending on the sign and magnitude of magnetostriction constant. As is illustrated in Fig. 2, little effect of applied tensile stress is observed in the samples with negative magnetostriction. In the alloys with positive λ_s the domain structure substantially changes near some critical stress σ_c , where the *planar* anisotropy changes to the *uniaxial* one with the easy axis along the ribbon (Fig.3). The transversal stripe domains first change to antiparallel longitudinal stripes, some of which finally extend to a single domain with residual cigar-like domains of the opposite orientation. This is in good agreement with the behavior of hysteresis loops.

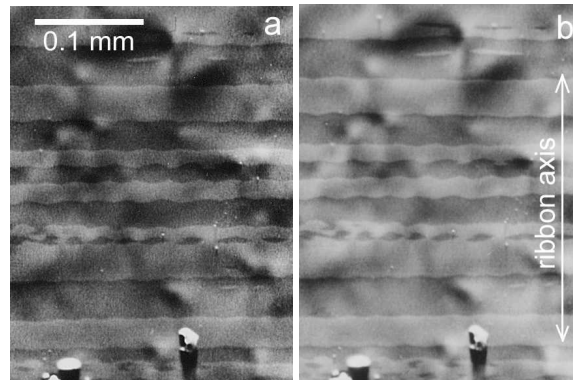


Fig. 2. Domain structures of stress-annealed $\text{Co}_{69}\text{Fe}_2\text{Cr}_7\text{Si}_8\text{B}_{14}$ ribbon (350°C/1 h./400 MPa).
a) $\sigma = 0$, b) $\sigma = 450$ MPa (transversal contrast).

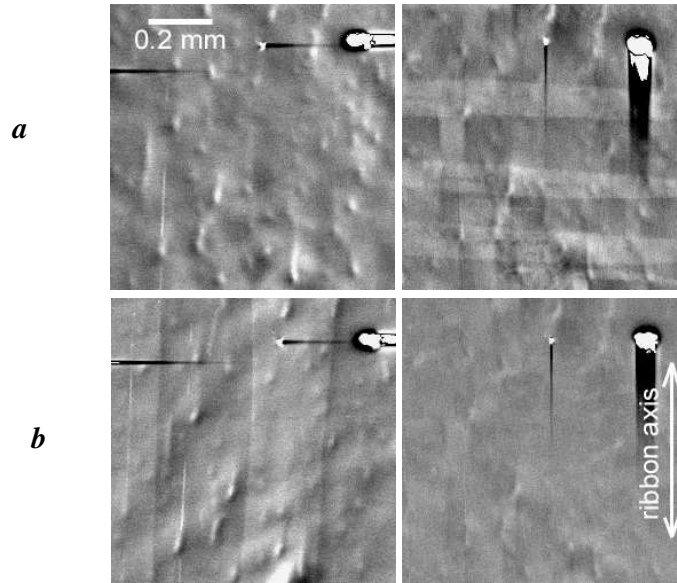


Fig. 3. Domain structures of stress-annealed $\text{Co}_{63}\text{Fe}_8\text{Cr}_7\text{Si}_8\text{B}_{14}$ ribbon ($350^\circ\text{C}/1\text{ h.}/300\text{ MPa}$).
 a) $\sigma = 0$, b) $\sigma = 52\text{ MPa}$ (left – transversal contrast, right – longitudinal contrast).

The hysteresis loops of two alloys ($x = 2$ and 4), measured at various applied stress are shown in Fig. 4. The loops are linear practically up to 90% of saturation magnetization and show very small coercive force. This indicates that the magnetization reversal takes place only by magnetization rotation. The effective anisotropy field is calculated from the formula $H_K = J_s/\chi_i$, where χ_i is the initial susceptibility. The slope of the hysteresis loop changes with the applied tensile stress and the anisotropy field well satisfies the linear dependence

$$H_K = H_{K0} - 3 \frac{\lambda_s}{J_s} \sigma, \quad (1)$$

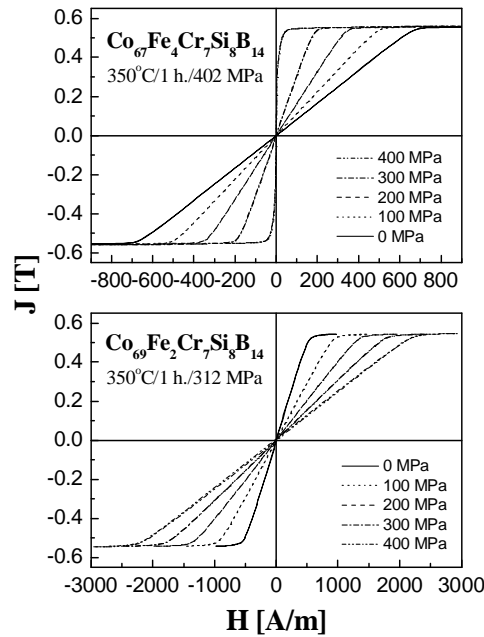


Fig. 4. Effect of applied stress on hysteresis loops of stress-annealed CoFeCrSiB ribbons.

where H_{K0} is the anisotropy field induced by stress-annealing (see Fig. 5). For $\lambda_s < 0$ the anisotropy field increases without any limit, while for $\lambda_s > 0$ it decreases and reaches zero at the critical applied stress $\sigma_c = J_s H_K / (3\lambda_s)$. At this stress the transversal anisotropy changes to the longitudinal one, which is accompanied by the change of domain structure, as described above. Because stress-annealing induces quite a large transversal anisotropy ($H_{K0} > 0$), λ_s of stress-annealed samples can be calculated from Eq. (1). The compositional dependence of λ_s for the samples annealed under stress of 400 MPa is shown in Fig. 6 together with the $\lambda_s < 0$ values of the as-quenched ribbons. As can be seen, the magnetostriction constant is a linear function of x . A slight increase of λ_s after stress-annealing is caused by the short-range order relaxation of the amorphous structure [8].

By assuming that the transversal anisotropy ensures magnetization process prevailing by the magnetization rotation, the dependence of permeability obtained from Eq. (1) is given by

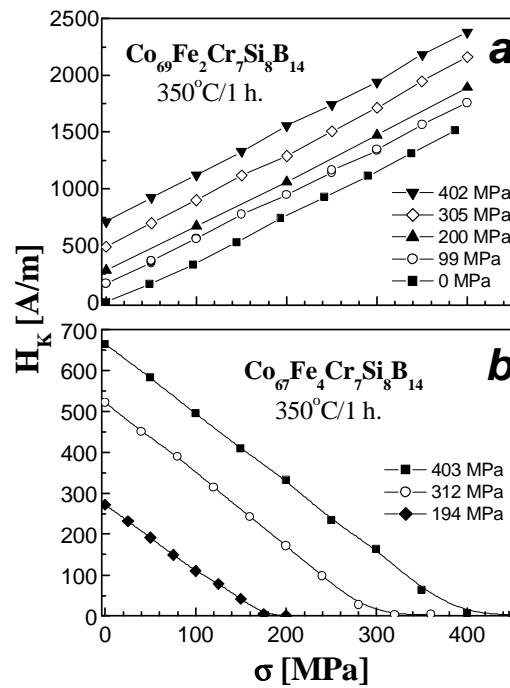


Fig. 5. Effective anisotropy field as a function of applied stress for the stress-annealed ribbons. *a*) alloy with negative magnetostriction, *b*) alloy with positive magnetostriction.

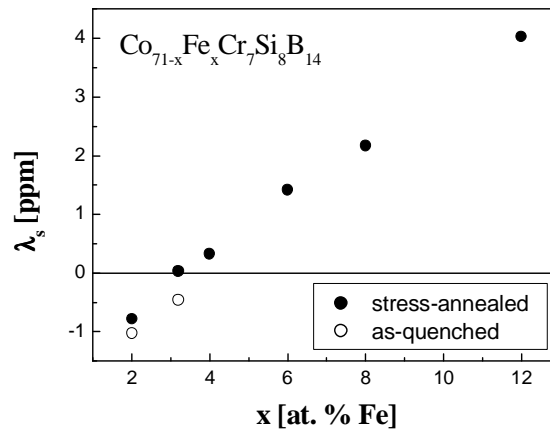


Fig. 6. Saturation magnetostriction constant of as-quenched and stress-annealed (350°C/1 h./400 MPa) amorphous CoFeCrSiB ribbons.

$$\mu = \mu_0 + \frac{J_s^2}{J_s H_{K0} - 3\lambda_s \sigma}, \quad (2)$$

where μ_0 is the permeability of vacuum. Because μ_0 is negligible with respect to the second term on the right hand side of Eq. (2), the reluctivity (μ^{-1}) is nearly linear function of applied stress. The measurements of AC permeability proved that the linear dependence is well fulfilled in the stress-annealed ribbons $\text{Co}_{69}\text{Fe}_2\text{Cr}_7\text{Si}_8\text{B}_{14}$ and $\text{Co}_{67}\text{Fe}_4\text{Cr}_7\text{Si}_8\text{B}_{14}$. This behavior is advantageous for the construction of strain sensors, where amorphous ribbon is used as the core of an induction coil.

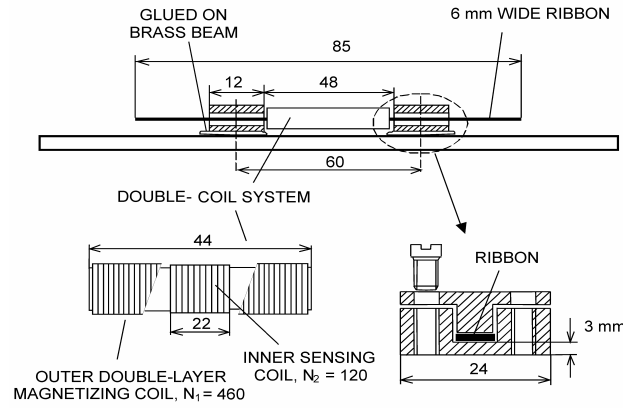


Fig. 7. Two-coil strain sensor. (Dimensions are shown in mm).

4. Strain sensor

The high strain sensitivity of permeability and low hysteresis of stress-annealed ribbons, provide large „figure of merit“ and a good reproducibility of strain measurements. The $\text{Co}_{71-x}\text{Fe}_x\text{Cr}_7\text{Si}_8\text{B}_{14}$ alloys with $x = 2$ and 4 were tested in the prototype of two-coil strain sensor shown in Fig. 7. The sensor is strained by means of the brass beam, which is fixed at both ends and bent by a force applied to its center. The exciting coil is supplied by a power operational amplifier at a frequency of 5 kHz. Both, the waveform and the amplitude of exciting current are controlled by a feedback loop, which ensures that the voltage U_2 induced in the pick-up coil remains sinusoidal and constant when the flexure of the beam is changed. The exciting current I_{mag} as a function of the strain ε of the brass beam upper surface is shown in Fig. 8. The gauge „figure of merit“, defined as $K = |\Delta I_{mag}|/(I_{mag \min} \varepsilon_{\max})$, is also shown in the figure. Both alloys show good current-strain characteristics. Though, the sensitivity obtained for the $\text{Co}_{67}\text{Fe}_4\text{Cr}_7\text{Si}_8\text{B}_{14}$ alloy is smaller than that of $\text{Co}_{69}\text{Fe}_2\text{Cr}_7\text{Si}_8\text{B}_{14}$ alloy, the characteristic of the former displays much better linearity.

The disadvantage of positive magnetostriction materials is, however, that they can work only up to the critical strain $\varepsilon_c = \sigma_c/E$, which depends on the magnetostriction constant and the induced anisotropy field H_{K0} .

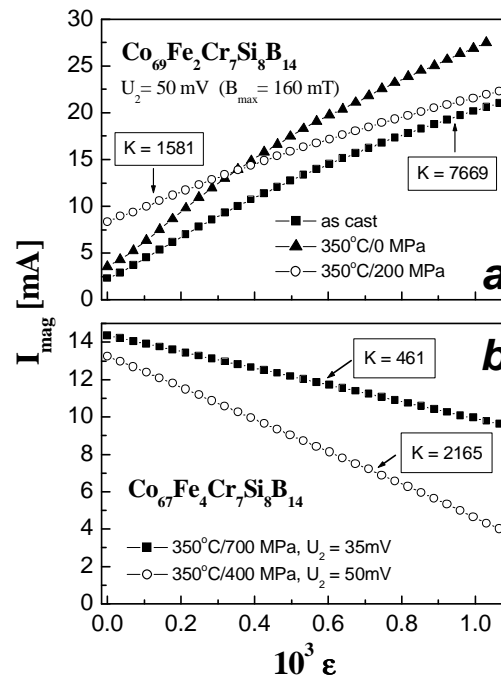


Fig. 8. Exciting current of the two-coil strain sensor vs. applied strain. *a*) material with $\lambda_s < 0$ in the as-quenched and stress-annealed states; *b*) stress-annealed material with $\lambda_s > 0$.

5. Conclusions

The obtained results show the possibility to use the amorphous Co-rich alloys CoFeCrSiB with low magnetostriction as potential candidates for application in civil engineering strain sensing. The transversal magnetic anisotropy induced by stress-annealing can be used to improve the sensor characteristics. This thermal treatment gives the possibility to use the positive magnetostriction materials with high linearity of transfer characteristics and wide range of measured strain.

Acknowledgement

The work was supported by the NATO SfP Project No. SfP-973649 “Quenched Materials”.

References

- [1] A. Hernando, M. Vázquez, J. M. Barandiarán, J. Phys. E: Sci. Instrum. **21**, 1129 (1988).
- [2] M. Wun-Folge, H. T. Savage, A.E. Clark, Sensors and Actuators **12**, 323 (1987).
- [3] J. M. Barandiarán, J. Gutierrez, Sensors and Actuators **A 59**, 38 (1997).
- [4] J. D. Livingston, Phys. Stat. Sol. **A 70**, 591 (1982).
- [5] O. V. Nielsen, IEEE Trans. Magn. MAG-21, 2008 (1985).
- [6] K. Jurek, K. Závěta, JEOL News **26E**, 17 (1988).
- [7] K. Závěta, L. Kraus, K. Jurek, V. Kamberský, J. Magn. Magn. Mater. **73**, 334 (1988).
- [8] A. Hernando, M. Vázquez, V. Madurga, H. Kronmüller, J. Magn. Magn. Mater. **49**, 161 (1983).